

# Damage quantification in TBCs by photo-stimulated luminescence spectroscopy

J.A. Nychka\*, D.R. Clarke

*Department of Materials, College of Engineering, University of California Santa Barbara, Santa Barbara, CA 93106-5050, USA*

---

## Abstract

A procedure is described for assessing the extent of damage in an electron beam vapor deposited (EBPVD) thermal barrier coating (TBC) based on the quantitative analysis of its photo-stimulated luminescence spectrum. In contrast to purely statistical fitting procedures, the analysis procedure uses experimental calibrations of the effect of stress on the principal features of a luminescence spectrum. Luminescence spectra from a thermally cycled TBC are used to illustrate the procedure and derive estimates of the thermal cycling induced damage. © 2001 Elsevier Science B.V. All rights reserved.

*Keywords:* Photo-stimulated luminescence spectroscopy; Thermal barrier coating; Physical vapor deposition

---

## 1. Introduction

There is a real need for non-destructive tools to evaluate whether a thermal barrier coating is damaged and, on the basis of the damage detected, determine how much life remains before failure occurs. Once the TBC has buckled or spalled it can generally be seen optically, but it is essential to develop a tool capable of detecting damage evolution prior to it reaching the critical buckling size. Thus, it is a pre-requisite that the non-destructive tool be able to probe through the thickness of the thermal barrier coatings to detect any damage. One particularly promising method is photo-stimulated luminescence spectroscopy (PSLS) since it is both non-destructive and produces a direct measure of local elastic strain energy in the thermally grown oxide (TGO).

Originally, it was anticipated that the shift in the R line luminescence spectrum [1,2] obtained by laser photostimulation from Cr<sup>3+</sup> ions incorporated into the TGO would be a reliable indicator of the life of a TBC.

However, as a larger body of experience has been gained, it is becoming clear that whilst the luminescence shifts are a reliable measure of the residual stress in the TGO, they are not as reliable as a measure of damage or damage accumulation. Instead, as envisaged and originally shown by Clarke et al. [3], for a number of TBCs, the width and shape of the luminescence peaks provides more reliable information on the presence of damage in the probed volume. This requires that the luminescence spectrum recorded from a thermal barrier coating be analyzed by a deconvolution procedure to obtain the information contained within the spectrum. There are two approaches to this spectral analysis. One is to recognize that the spectrum contains a series of R1–R2 peaks and obtain the best statistical fit to the measured luminescence spectrum, as assessed, for instance, by the chi-square ( $\chi^2$ ) value of the fit. The other is to use previously established calibration data from alumina under a variety of stress states to constrain the data fitting so as to obtain data about the type of damage. This is conveniently referred to as ‘physically-based’ fitting in the following sections.

In cases where the TBC is heavily damaged, the spectrum clearly contains additional distinct peaks. In such cases, the presence of the additional peaks is a

---

\* Corresponding author. Tel.: +1-805-893-3559; fax: +1-805-893-8971.

E-mail address: jnychka@engineering.ucsb.edu (J.A. Nychka).

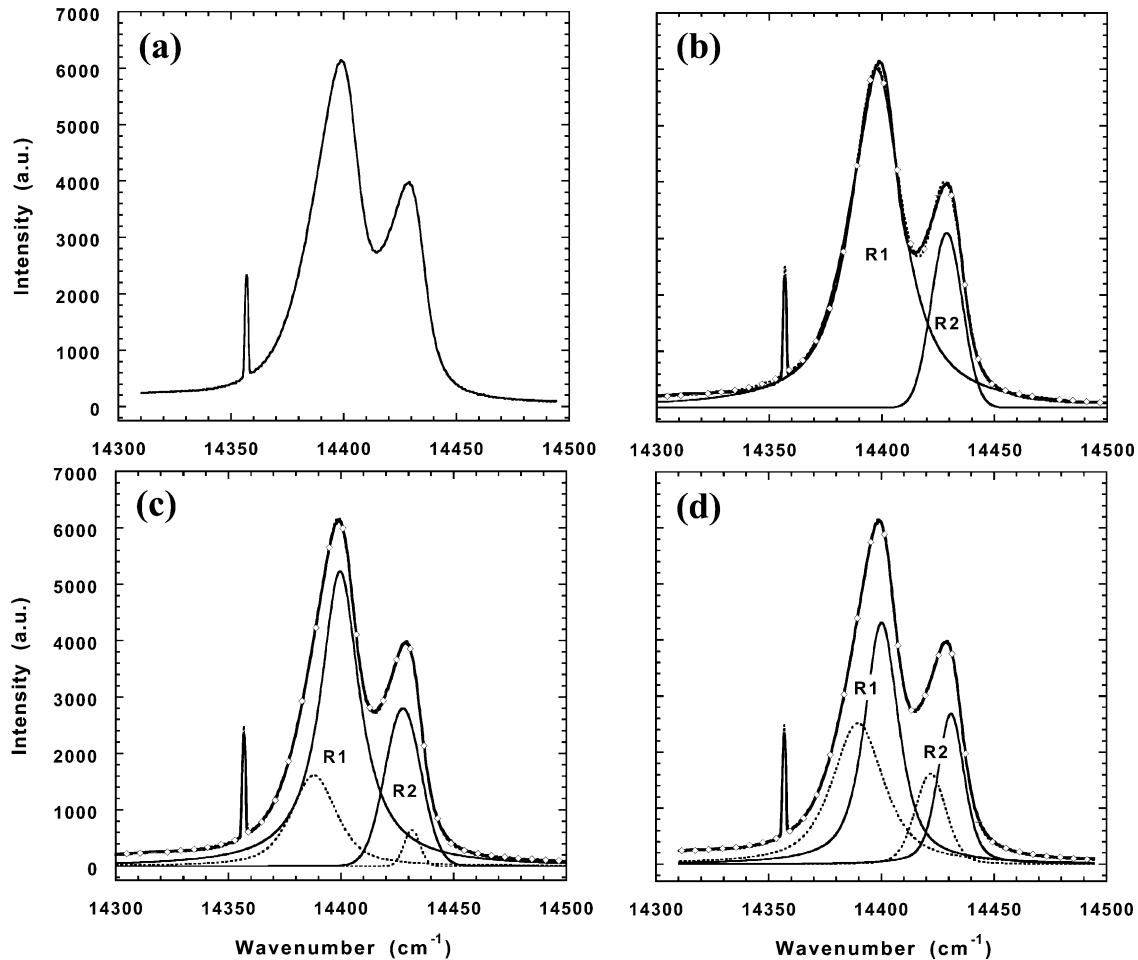


Fig. 1. PSL spectrum taken from a thermally cycled EB-PVD TBC (a), and three alternative deconvolutions: (b) two peaks using a statistical fit, (c) four peaks using a statistical fit and (d) four peaks using a physically-based fit. Fitting parameters and statistical deviation for the deconvolutions are shown in Table 1. Markers indicate the summation of the convolutions (closely overlapping experimental spectrum). The two doublets in (c) and (d) are indicated by the solid and dashed lines. The deconvolution in 1(b) is a poor match to the spectrum (the dashed convolution line is seen separated from the solid experimental spectrum line). The fit in 1(c) shows low statistical variation with the spectrum, but does not maintain the physics of the luminescence. 1(d) is concluded to be the correct depiction of the stress in the TGO because it has low statistical variation and maintains the physics of the R line luminescence.

straightforward indication of damage in the TBC, but experience suggests that wholesale failure of the coating is then imminent. To be a practical tool, it is essential that the damage be detected at an earlier stage when the luminescence from the damaged region is masked by the stronger luminescence from the surrounding undamaged regions. It is for the analysis of the early stages of damage that it is important to have a physically based procedure for analyzing the luminescence spectrum. To illustrate the physically-based approach, we consider the luminescence spectrum in Fig. 1a recorded from an electron-beam vapor deposited TBC after thermal cycling. In contrast to spectra from highly damaged TBCs, the spectrum appears as a single doublet, suggesting that no damage has occurred. However, as will

be described, a quantitative physical analysis indicates that damage has indeed occurred.

## 2. Analysis

Our starting point is the piezospectroscopic relation. Over a wide range of stresses, a homogeneous stress,  $\sigma_{ij}$ , causes a linear shift in frequency,  $\Delta\nu$ , of the R lines from their stress-free frequency given by:

$$\Delta\nu = \Pi_{ij}\sigma_{ij} \quad (1)$$

where  $\Pi_{ij}$  is a first-order phenomenological tensor whose values have been determined experimentally [4]. (The repeated index notation is used here.) The luminescence lines recorded from an unstressed alumina

material have a mixed Gaussian–Lorentzian line shape as a result of thermal broadening and various instrumental factors. As a result, the measured line shape,  $\Phi(\nu)$ , can be represented by:

$$\Phi(\nu) = (1-L)I_{\max}e^{-(\nu-\nu_m/w)^2[4\ln(2)]} + L\frac{I_{\max}}{1+4\left(\frac{\nu-\nu_m}{w}\right)^2} \quad (2)$$

where the first term is the Gaussian component, the second is a Lorentzian component,  $L$  is the relative proportion of Lorentzian character,  $\nu_m$  is the frequency at the maximum intensity,  $I_{\max}$ , and  $w$  is the full width at half height. Therefore, for a homogeneously strained body, the luminescence line is unchanged in shape and merely shifted by a constant frequency,  $\Delta\nu$ .

For an *inhomogeneously* strained material, the shape of the luminescence peaks is changed and they typically become broader. The physical basis for analyzing the change in shape of the luminescence spectra is that the photon emission from each  $\text{Cr}^{3+}$  ion is independent of the other  $\text{Cr}^{3+}$  ions. Consequently, each ion acts as an independent strain sensor so the overall luminescence is the sum of the photons emitted by the individual  $\text{Cr}^{3+}$  ions. If there is a variation in strain, then the individual ions within the probed volume will each luminesce at slightly different frequencies and cause an apparent peak broadening. As a result, the peak broadening is generally proportional to the variation in stress within the probed volume. A general treatment that relates spectral shapes to spatial property distributions was developed a few years ago by Lipkin and Clarke [5]. If we assume that within the probed volume there are some regions that are damaged and others that are undamaged, the Lipkin–Clarke analysis can be reduced to an expression for the intensity as the integral over the probed volume of the luminescence from each of the individual regions,  $i$ :

$$I(\nu) \propto h \int_{-r_p}^{+r_p} \sum_i W_i \Phi[\nu\{\sigma_i\}] B(r) dr \quad (3)$$

where  $r_p$  is the probe radius,  $W_i$  represents the relative areas of regions,  $i$ , for instance the damaged and undamaged regions,  $B(r)$  represents the spatial variation in intensity of the probe, and the oxide thickness is  $h$ .

The form of Eq. (3) suggests that the luminescence peak can be fitted with a number of individual spectra, each corresponding to the area fraction of differently stressed regions within the probed volume and the average stress in those regions, superimposed. If the TGO is undamaged, the luminescence peaks can be fit, as is standard practice, by a single doublet representing the R1/R2 peaks of  $\text{Cr}^{3+}$  doped alumina shifted in proportion to the stress in the TGO. This would correspond to the homogeneous case with  $i=1$  in Eq. (3). When damage occurs, the luminescence peaks can no

longer be fit with a single R1/R2 doublet. Instead, more than one peak is required for fitting with the number of peaks,  $i$ , their weighting,  $W_i$ , and their centroid frequency,  $\nu_i$  being variable in the fitting procedure. Such an analysis has recently been applied to TBCs by Peng and Clarke [6].

### 3. Fitting parameters

The procedure for fitting a spectral peak with a combination of peaks is a standard feature of many commercial software packages for spectral analysis, such as the commercial GRAMS package. In addition, a number of numerical algorithms have been developed for spectral peak fitting. The one we have used most extensively at UCSB is one based on the Levenberg–Marquardt non-linear peak method [7].

The stress dependence of the luminescence from various forms of alumina, containing  $\text{Cr}^{3+}$  ions, has been studied in numerous publications [1,3,8–10], since the application of stress was first used to study the details of the electronic transitions in ruby. Most studies have been of the shift in luminescence frequency under rather simple states of stress, such as uniaxial and hydrostatic stress, but recent work has extended our knowledge to the stress dependence of other characteristic features of the R1 and R2 luminescence spectrum as will be described.

#### 3.1. Frequency shift

The frequency of the R1 and R2 lines is sensitive to stress, temperature and concentration of  $\text{Cr}^{3+}$ . At room temperature (22°C), the frequencies of the R lines from stress-free, single crystals of sapphire containing 0.05 wt.% Cr ruby are 14433.44  $\text{cm}^{-1}$  for R2 and 14403.44  $\text{cm}^{-1}$  for R1. These values decrease with increasing temperature by 0.134  $\text{cm}^{-1}$  °C and 0.144  $\text{cm}^{-1}$  °C, respectively, for the R2 and R1 lines [4], so it is necessary in analyzing luminescence spectra to correct for temperature. (Typically, we measure the room temperature at the same time as recording the luminescence spectra so as to correct for temperature.) There is also known to be an effect of chromium concentration on the frequency of both the R1 and R2 lines [11], but since it is extremely difficult to determine the chromium concentration independently, we usually seek to compare the measured luminescence frequency to that recorded from a spalled fragment of the oxide to obtain the ‘stress-free’ frequency. Since the chromium concentration will not have changed significantly when the oxide fails, it is assumed that the only change in frequency is due to release of the stress in the spalled fragment. In the event that failure has not yet occurred, a sapphire standard (0.05 wt.% chromium) is used to obtain an estimate of the stress free frequency. TGOs typically

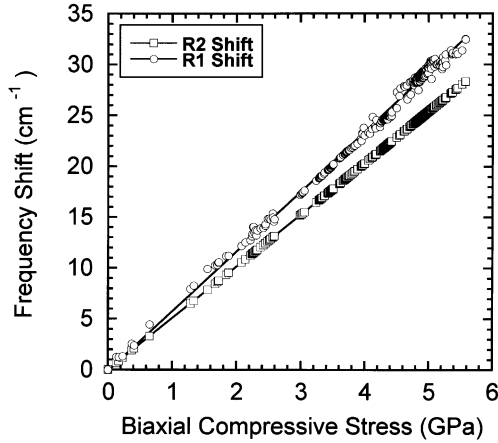


Fig. 2. Frequency shifts of the R1 and R2 lines taken from oxides grown on various FeCrAl alloys. Notice that R1 is linear, but with a much larger stress dependence than R2.

have slightly more chromium than does sapphire: the stress free frequency of the studied TGOs has been found to be  $\sim 14433.64 \text{ cm}^{-1}$  for R2, and  $\sim 14403.64 \text{ cm}^{-1}$  for R1. Sample-to-sample variations are negligible and need not be considered so long as the same material system is being considered.

The effect of uniaxial stresses along different crystallographic directions and the effect of hydrostatic pressure have been systematically studied on sapphire crystals containing typically 0.05 wt.% chromium. From these systematic experiments, the values of the piezospectroscopic coefficients have been determined [4]. Assuming that the distribution of grains in a thermally grown oxide are randomly oriented then the frequency shift when the TGO is under biaxial stress,  $\sigma_B$ , would be given by:

$$\Delta\nu = \frac{2}{3}(\Pi_{11} + \Pi_{22} + \Pi_{33})\sigma_B \quad (4)$$

where the sums of the coefficients have been found to be  $7.61$  and  $7.59 \text{ cm}^{-1} \text{ GPa}$  for R2 and R1, respectively [4].

### 3.2. Peak separation

Experiments under hydrostatic pressure have indicated that the separation between the R1 and R2 peaks is  $30.0 \text{ cm}^{-1}$  at room temperature and does not change with pressure. However, when the stress state is not hydrostatic, the peak separation does depend on stress and the stress state.

The frequency shift as a function of residual biaxial compressive stress is shown in Fig. 2 for various thin films grown on FeCrAl alloys. The residual stress was calculated using the experimental values of the R2 shift and the known piezospectroscopic coefficients [Eq. (4)].

The R1 shift was plotted as a function of the stress as calculated from the R2 shift. Using these data, it can be anticipated that under biaxial compression, the R1 and R2 peaks will separate by an amount of  $0.82 \text{ cm}^{-1} \text{ GPa}$  with increasing biaxial compressive stress in the range 0.0–5.5 GPa.

### 3.3. Intensity ratio

The underlying physics would suggest that the ratio of intensities of the R1 and R2 lines would be only weakly dependent on temperature and pressure. This was confirmed by Munro et al. [12] who found the intensity ratio of the R lines (R2/R1) varied by  $-0.00047^\circ\text{C}^{-1}$  and  $-0.013 \text{ GPa}^{-1}$ , with temperature and pressure, respectively. Thus, for all practical purposes, the temperature dependence can be ignored. The value of the ratio does, however, depend on the crystallographic orientation with respect to the polarization of the laser used to stimulate the luminescence. This can be quite a large effect for single crystals but not for polycrystalline alumina, such as found in TGOs where the R2/R1 value ranges from 0.52 to 0.71 (Fig. 3). This range is most likely due to the presence of weak texture. Both the mean and median values of the intensity ratio for the data in Fig. 3 were 0.60 with a S.D. of 0.02. The bar on the ordinate shows the value of single crystal *c*-axis sapphire. In some cases, sub-micron films have an inverted R2/R1 value, but this behavior is not fully understood.

### 3.4. Peak shape

As mentioned in Section 2, the R1 and R2 luminescence lines can be modeled as a mixture of Lorentzian and Gaussian functions [1,6,12]. For a stress-free sap-

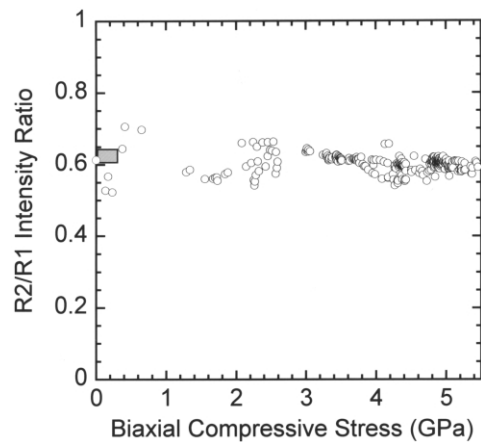


Fig. 3. Intensity ratio (R2/R1) from oxides on various FeCrAl alloys as a function of the biaxial compressive stress (R2 frequency shift). The bar on the ordinate indicates the intensity ratio of stress free single crystal *c*-axis sapphire.

phire single crystal oriented in the  $c$  direction the  $L$  and  $G$  fractions were found to lie in a fairly narrow range:  $L=0.70$ – $0.85$  for R2, and  $L=0.90$ – $0.99$  for R1 ( $G=1-L$ ). Stressed polycrystalline films were found to have a lower  $L$  fraction:  $L=0.40$ – $0.70$  for R2, and  $L=0.70$ – $0.90$  for R1. This decrease in  $L$  fraction seems to be concomitant with peak broadening due to crystal misorientation and strain gradients in the film.

### 3.5. Broadening

Broadening of the R-lines is usually due to temperature and the presence of variations in strain within the luminescing region. At room temperature, the R lines of a 0.05-wt.% chromium ruby have full width at half maximum (FWHM) values of 8.3 and 11.2  $\text{cm}^{-1}$  for R2 and R1, respectively. Temperature effects on the FWHM were not investigated for this study, but may be found in He and Clarke [4]. In general, the R2 line is 0.75 times as broad as the R1 line, but ranges from 0.70 to 0.90 in polycrystalline films.

### 3.6. Guidelines and procedure for fitting

Having a knowledge of how the principal features of the luminescence R1 and R2 lines vary with stress, it is now possible to use these data to constrain the fitting of luminescence spectra.

As the preceding data indicates, there is always some variability in the fitting parameters with stress. In part, this is a natural consequence of variations in crystal texture, grain size, and stress within the scale. These variabilities can be incorporated into the software package used for the curve fitting (GRAMS).

The procedure we have adopted for fitting a spectrum is an iterative one, as follows. The first parameter specified is a range for the  $L$  fraction: 0.40–0.70 for R2, and 0.70–0.90 for R1. Once the computer has found the best fit, the R2 peak position is viewed, and is converted into a stress. Knowing the magnitude of the compressive stress helps to determine what the peak separation should be; the separation should scale as  $0.82 + 0.10 \text{ cm}^{-1} \text{ GPa}$ . Next, the intensity ratio R2/R1 is evaluated to determine if it falls within the range 0.55–0.63, and the FWHM ratio R2/R1 falls within 0.70–0.90. After performing these checks, if the parameter ranges are not met, the calculated peaks are shifted so that the separation is consistent with the computed R2 shift, and the statistical deviation is as close to zero as possible. Then more iterations are performed until the solution converges and the parameters are consistent.

Spectra from TBCs are typically asymmetric and can be deconvoluted into an intense doublet, and a less intense doublet. The less intense doublet tends to be broader due to the fact that it approximates different

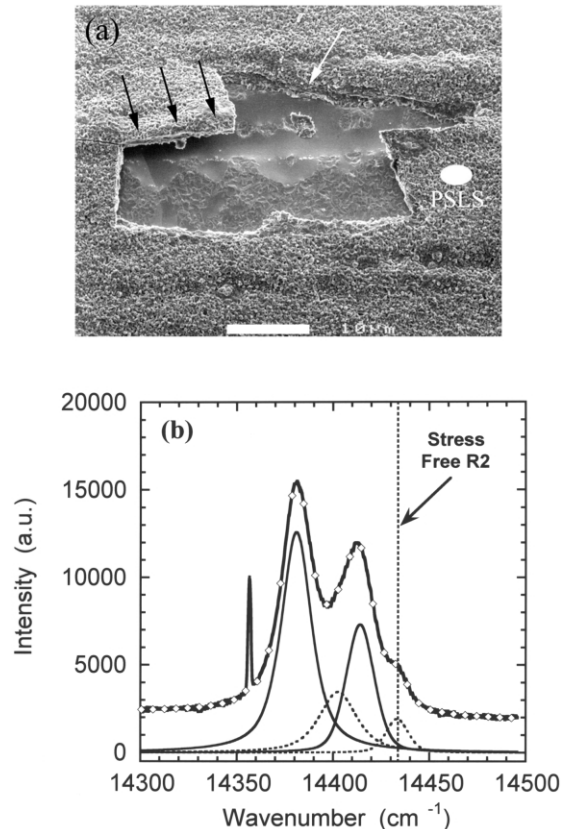


Fig. 4. A spalled area of TGO grown on a Kanthal A-1 wire, 1100°C for 16 h, (a), and a deconvoluted PSL spectrum from the same wire, (b). The white spot in (a) corresponds to the size of the area, and position where the spectrum in (b) was taken. The black arrows indicate an area of debonded oxide, while the white arrow indicates oxide remaining in contact with the metal. (b) Markers indicate the summation of the convolutions. The two doublets are indicated by the solid and dashed lines, where the solid and dashed lines correspond to intact oxide and debonded oxide, respectively.

strain states. For this reason, lower intensity doublets typically have the lowest values of  $L$  fraction:  $L=0.20$ – $0.40$  for R2, and  $L=0.40$ – $0.70$  for R1, while the higher intensity doublets have the same  $L$  fraction as normal films above. The remaining procedure for determining the other parameters is the same for both sets of doublets.

## 4. Damage evaluation

In this section, we will demonstrate the difference between fitting with and without using any guidelines for the luminescence characteristics of TGOs, and the information that can be obtained. To illustrate the procedure, we present the luminescence spectra, and their analysis, from an oxide where the damage is visible and the individual spectra were obtained from identifiable regions of intact and buckled oxide. The material is an

Table 1  
Fitting parameter and  $\chi^2$  values for spectral deconvolutions taken from an EBPVD TBC

Spectrum	R Line <sup>a</sup>	$\Delta\nu^b$ ( $\text{cm}^{-1}$ )	$\sigma_B^c$ (GPa)	Intensity ratio R2/R1	FWHM R2/R1	L Fraction	$\nu_{R1} - \nu_{R2}$ ( $\text{cm}^{-1}$ )	$\chi^2$	Damage proportion <sup>d</sup> (%)
(b)	R2	4.59	0.90	0.51	0.61	0.00	31.1	1.434	N/A
	R1	5.67							
(c)	R2a	5.75	1.13	0.54	0.90	0.02	28.0	2.208	20
	R1a	3.73							
	R2b	1.75	0.34	0.40	0.36	0.00	43.6		
	R1b	15.33							
(d)	R2a	2.45	0.48	0.62	0.77	0.40	30.8	0.041	49
	R1a	3.23							
	R2b	11.45	2.26	0.64	0.60	0.20	32.3		
	R1b	13.73							

<sup>a</sup> The solid line doublet in Fig. 1 is labeled as Ra, and the dashed line doublet as Rb.

<sup>b</sup> Frequency shift after temperature and argon reference correction.

<sup>c</sup> Stress calculated from R2 shift using the relation  $\sigma_B = \Delta\nu \cdot 0.197$ .

<sup>d</sup> Damage proportion is defined as the area percentage of the damaged peaks (R1 and R2) to the total area of both deconvoluted doublets (R1 and R2 of all deconvoluted luminescence peaks). The damaged regions correspond to the peaks with the lowest frequency shift. Damage proportion =  $(\sum \text{Area of damaged R peaks}) / (\sum \text{Area all R peaks})$ .

alumina scale on a FeCrAlY (Kanthal A-1). After oxidation for 16 h at 1100°C and subsequent cooling, local spallation occurs, as shown in Fig. 4. A luminescence spectrum was recorded near the edge of a similar spall (the white spot in the figure corresponds to the probe size). The deconvoluted spectrum (Fig. 4b), performed in accordance to the outlined guidelines, demonstrates that there are at least two distinct stress states present within the probed volume as seen by the difference in the frequency shifts of the R2 peaks. The oxide in contact with the metal shows a high value of R2 frequency shift as it is under a large residual compression (3.7 GPa), while the debonded oxide shows no R2 frequency shift since it is no longer in contact with the metal.

Returning now to Fig. 1, the spectrum from the thermally cycled TBC is shown along with three alternative deconvolutions. The R1 and R2 labels show the regions where the deconvoluted R lines are located. The solid and dashed deconvoluted peaks correspond to different doublets. The diamond markers with a dashed line correspond to the summation of the deconvoluted peaks. The argon reference line was fitted in each case, but is not shown in the figure. The fitting parameters and  $\chi^2$  values are listed in Table 1.

Fig. 1b was fit with a single doublet, specifying no parameters and allowing the computer algorithm in GRAMS to perform as many iterations as needed to obtain a convergent solution with a constant  $\chi^2$  value. The fit does not fully reproduce the peaks of the R lines, so the peak positions are incorrect. Realizing that the spectrum is asymmetric, it was then assumed that it

contains two doublets. Fig. 1c was, therefore, fit with two doublets, without specifying any physical constraint on the fitting parameters, and iterated in the same fashion as for Fig. 1b. While the fit appears to overlap the experimental spectrum rather well, the dashed line doublet has a very large peak separation (42  $\text{cm}^{-1}$ ), the shapes of the peaks are inconsistent, and the FWHM ratio of the dashed doublet is very low, indicating that this fit is inconsistent with the known stress dependencies. Fig. 1d was then fit according to the procedural guidelines in the previous section. This fit is much more

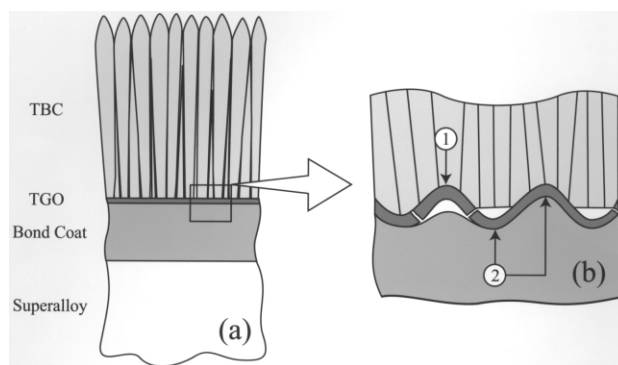


Fig. 5. Schematic of types of damage associated with thermal cycling of EB-PVD TBCs. (a) Cross section view showing the presence of the TGO between the TBC and the bond coat. (b) Magnified view of TBC-TGO-Bond Coat structure after thermal cycling. Local separations between the TGO and bond coat form, leaving the oxide attached only to the TBC (region 1); intact oxide may or not be attached to the TBC (region 2).

Table 2  
Frequency shifts, biaxial stress, and damage proportion for three similarly coated EBPVD TBC samples as a function of cycling time

Sample	Number of cycles	R Line	$\Delta\nu$ (cm <sup>-1</sup> )	$\sigma_B$ (GPa)	Damage proportion (%)
As-coated	0	R2a	6.07	1.20	48
		R1a	7.35		
		R2b	14.66	2.81	
		R1b	18.40		
A	100	R2a	8.64	1.70	72
		R1a	9.67		
		R2b	20.47	4.03	
		R1b	24.84		
B	292	R2a	2.45	0.48	49
		R1a	3.23		
		R2b	11.45	2.26	
		R1b	13.73		

Calculations of biaxial stress and damage proportion were performed as indicated in Table 1.

consistent and also shows the lowest  $\chi^2$  value. The less intense doublet has a peak separation slightly outside the anticipated limits, and a low FWHM ratio, which indicates that there might yet be another weak doublet present.

The stresses obtained from the deconvolution in Fig. 1d indicate that there are at least two regions under very different biaxial compression: one at an average of 0.48 GPa and another at an average of 2.26 GPa. Such different stresses are consistent with observations of damage in the form of local TBC–TGO and TGO–bond coat interface separations (Fig. 5). A stress of  $\sim 0.50$  GPa is consistent with the thermal expansion mismatch between zirconia TBC and dense alumina, and suggests that it comes from where the TGO may have completely separated from the bond coat (Fig. 5, region 1). The higher stress value is most likely due thermal expansion mismatch between the intact TGO and the grit blasted bond coat surface (Fig. 5, region 2).

Assuming that the proportion of damaged to undamaged regions is given by the ratio of the peak areas

under the R lines, the damage proportion can be calculated, as shown in Table 1. For further illustration, Table 2 illustrates additional results from the analysis of similarly processed TBCs that have been subjected to thermal cycling.

## 5. Summary

A physically-based analysis procedure of PSL spectra from thermally grown alumina thin films under biaxial stress has been developed. This procedure is a promising technique to quantify the amount of damage in TBCs. However, it should be noted that there remains a need to account for effects of internal reflections, such as at cracks and local separations before one can completely specify the physical proportion of damaged to undamaged regions under the TBC. This type of calibration is underway.

## Acknowledgements

This work was supported through the DOE-AGTSR program. The authors wish to thank Dr K.S. Murphy, Howmet Corporation, for supplying thermally cycled TBC samples, and to Dr V.K. Tolpygo for insightful discussions.

## References

- [1] D.M. Lipkin, D.R. Clarke, *Oxid. Met.* 45 (1996) 267.
- [2] R.J. Christensen, D.M. Lipkin, D.R. Clarke, K.S. Murphy, *J. Appl. Phys. Lett.* 69 (24) (1996) 3754.
- [3] D.R. Clarke, R.J. Christensen, V.K. Tolpygo, *Surf. Coat. Technol.* 94–95 (1997) 89.
- [4] J. He, D.R. Clarke, *J. Am. Ceram. Soc.* 78 (5) (1995) 1347.
- [5] D.M. Lipkin, D.R. Clarke, *J. Appl. Phys.* 77 (1995) 1855.
- [6] X. Peng, D.R. Clarke, *J. Am. Ceram. Soc.* 83 (5) (2000) 1165.
- [7] D.W. Marquardt, *J. Soc. Ind. Appl. Math* 11 (1963) 431.
- [8] L. Grabner, *J. Appl. Phys.* 49 (2) (1978) 580.
- [9] Q. Ma, D.R. Clarke, *J. Am. Ceram. Soc.* 76 (6) (1993) 1433.
- [10] Q. Ma, D.R. Clarke, *Acta Metall. Mater.* 41 (6) (1993) 1817.
- [11] A.A. Kaplyanskii, A.K. Przhvuskii, R.B. Rozenbaum, *Soviet Phys. Solid St.* 10 (8) (1969) 1864–1868.
- [12] R.G. Munro, G.J. Piermarinin, S. Block, W.B. Holzapfel, *J. Appl. Phys.* 57 (2) (1985) 165.